Silicon Nano-Photonics Design of Mach Zehnnder Interferometer with Temperature Variation Impact

Muharrem Drebi
University of Tripoli, Libya
m.drebi@uot.edu.ly

Abstract – This paper is based on a design submitted as part of the requirements for Silicon Photonics professional course certification from University of British Columbia, Canada. It includes deign, simulation and layout for a Mach-Zehnder interferometer or MZI, it also includes fabrication of silicon photonic chip at the University of Washington Nanofabrication Facility, part of the National Science Foundations National Nanotechnology Infrastructure Network (NNIN). The fabricated silicon photonic chip was tested at the University of British Columbia under special automatic test setup arrangement with precision temperature control and sub micrometer laser alignment control. The design proposal includes five MZIs with different sizes. The optical waveguides of the MZIs are designed using 500nm width, 220nm height and with ΔL ranging from 30μm upto 100μm. Measurement data was received from UBC and compared with corner analysis.

Index Terms—**Silicon photonics, Photonic Integrated Circuits, Nano, SiEPIC, Interferometer, MZI, Lumerical, Klayout.**

I. Introduction

Silicon was recently being used to construct nano structures that can generate, manipulate and detect light. In hope for these structures namely photonic structures to function as photonic circuits similar to electronic circuits which generate, manipulate and detect electrons. Huge efforts and investments were made for the last ten years by companies to accelerate the developments of silicon nano photonic structures and to integrate more such structures or components into what is called Photonic Integrated Circuits or PICs. Also huge efforts are actively being made to combine and integrate electronic circuits with photonic circuits in a single Silicon Electronic-Photonic Integrated Circuits (SiEPIC). In this paper we are presenting the design and fabrication of one such useful silicon nano photonic structures, namely the Mach Zehnder Interferometer.

II. MZI Theory

Mach-Zehnder interferometer is a device that can detect the phase shift between two beams of light through constructive and/or destructive interference. This interference is created by making a difference in waveguide properties. In a balanced MZI, the difference is created by changing transmission coefficient β_1 and $\beta_2$through thermo-optical effect or through plasma dispersion and PN junction. The balanced MZI can be used to make an optical switch through thermo-optical effect or can be used to make an optical modulator through plasma dispersion and PN junction. In imbalanced MZI, the difference is created by changing the optical path length.

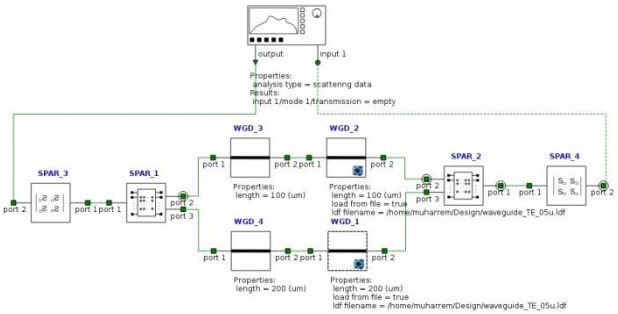

Figure 1. Lumerical INTERCONNECT Schematic for an imbalance MZI with ΔL=100μm, TE mode with α = 5.9dB/cm.

Lumerical INTERCONNECT Ref. [7] is used to create the schematic for an imbalance MZI as shown in Fig. 1, It is constructed using two Y-branches and two waveguides.

The light beam intensity is split equally through the first Y-branch, but then processed differently depending on the characteristics or the effective index, transmission loss and length of each waveguide creating a phase difference. Depending on the amount of the phase difference, the two waves are then combined constructively or destructively using a second Y-branch.

The general equation for the Mach-Zehnder interferometer is

$$I_o = \frac{I_i}{4}\left|\exp^{-i\beta_1 L_1 - \frac{\alpha_1}{2}L_1} + \exp^{-i\beta_2 L_2 - \frac{\alpha_2}{2}L_2}\right|^2. \quad (1)$$

Where α_1 and α_2 are propagation losses per length in each waveguide of the MZI branches, given the design constraints in the single etch process fabrication run used by this design, we can only make an imbalanced MZI by

using different waveguide lengths namely L_1 and L_2 and hence creating an optical path length difference.

$$\Delta L = L_1 - L_2. \quad (2)$$

III. MODELING AND SIMULATION

A. *Mode profile, n_{eff} and n_g*

First, Lumerical Mode Solution was used to model the waveguides and to generate simulation data for the effective index n_{eff}, group index n_g, transmission gain and waveguide loss. The mode profile is visually verified to make sure that the simulation boundary did not interfere with the waveguide structure and we can see from Fig. 2, that the field intensity has decayed to at least -10dB before reaching the boundary.

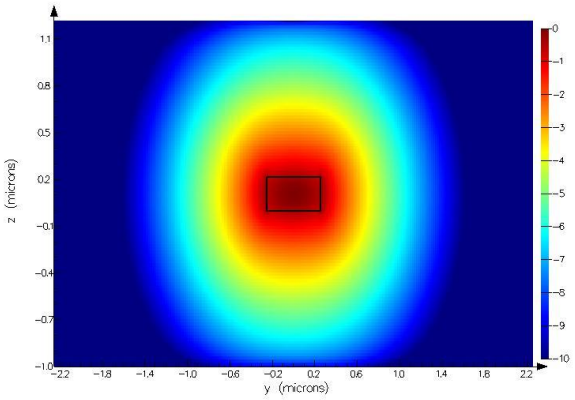

Figure 2. Lumerical Mode simulated TE mode profile, with 500nmx220nm waveguide.

The effective index n_{eff} and group index n_g verses λ are shown in Fig. 3, and Fig. 4, respectively. The n_g is about 4.181nm at $\lambda = 1550nm$ for TE mode and after verification, the simulation data was saved for the fundamental TE mode and TM mode as well.

B. *Compact model for n_{eff} and n_g*

Next, a compact model is generated by fitting the simulation data to a 2nd order polynomial. Both MATLAB curve fitting and Lumerical Mode Solutions were used to find coefficients of this polynomial equation for n_{eff}. The TE mode compact model for n_{eff} generated by Lumerical Mode Solutions is found as

$$n_{eff} = 2.44763 - 1.12923 * (\lambda - 1.55) - 0.0319043 * (\lambda - 1.55)^2. \quad (3)$$

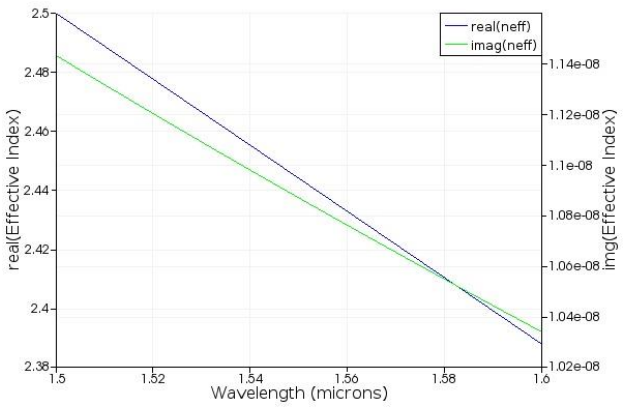

However, TE mode compact model for n_{eff} generated by MATLAB is found as

$$n_{eff} = 2.4476295 - 1.1292318 * (\lambda - 1.55) - 0.0318791 * (\lambda - 1.55)^2. \quad (4)$$

Figure 3. TE mode (98% polarization) effective index n_{eff} simulated using Lumerical Mode solutions, for 500nmx220nm waveguide.

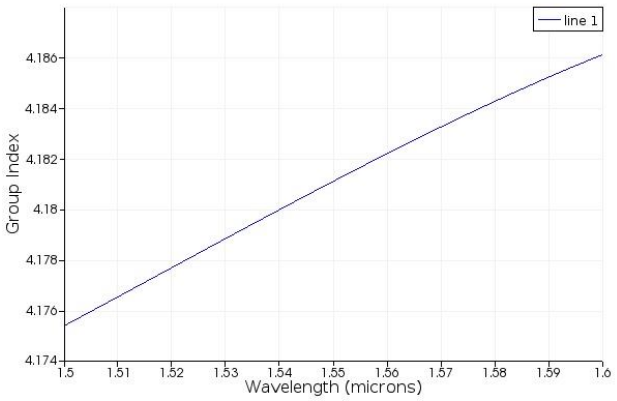

Figure 4. Group index n_g of the TE mode simulated using Lumerical Mode solutions, for 500nmx220nm waveguide.

As we can see, the difference is very small and hence we choose to use the results of Lumerical Mode solution curve fitting.

C. MZI transfer function

As discussed before in section II, we are implementing an imbalance MZI, where the effective index n_{eff} is kept the same $\beta_1 = \beta_2 = \beta$ and ΔL is varied. The transfer function of the MZI ignoring the propagation loss is

$$\frac{I_o}{I_i} = \frac{1}{2}[1 + \cos(\beta \Delta L)]. \quad (5)$$

Where

$$\beta(\lambda) = \frac{2\pi n_{eff}}{\lambda}. \quad (6)$$

n_{eff} from Fig. 3, is about 2.44 at $\lambda = 1550nm$, and the ΔL values for the five designed MZIs are

$$\Delta L = 30\mu m, 50\mu m, 70\mu m, 90\mu m, 100\mu m. \quad (7)$$

And if we include the loss, then the MZI transfer function is

$$T_{MZI} = \frac{I_o}{I_i} = \frac{1}{4}\left(1 + \exp^{-i\beta(\lambda)\Delta L}\right)^2. \quad (8)$$

Where

$$\beta(\lambda) = \frac{2\pi n_{eff}}{\lambda} + i\frac{\alpha}{2}. \quad (9)$$

The propagation loss α is determined through measurements and found to be 5.9dB/cm for TE mode and 1.2dB/cm for TM mode straight waveguides. And

since β is function of λ then the output of the MZI interferometer is a sinusoidal function of wavelength.
With MATLAB or lumerical INTERCONNECT the MZIs are simulated using the calculated compact model from section B, the simulated transmission spectrum(s) are plotted In Fig. 5, to Fig. 9, for $\Delta L=30\mu m$ upto $\Delta L=100\mu m$

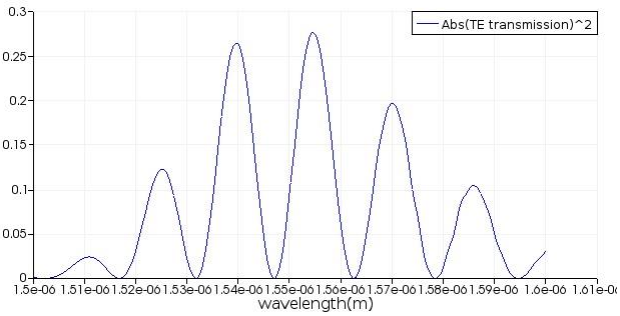

Figure 5. Spectrum of the imbalance MZI with $\Delta L=30\mu m$, TE mode for 500nmx220nm waveguide.

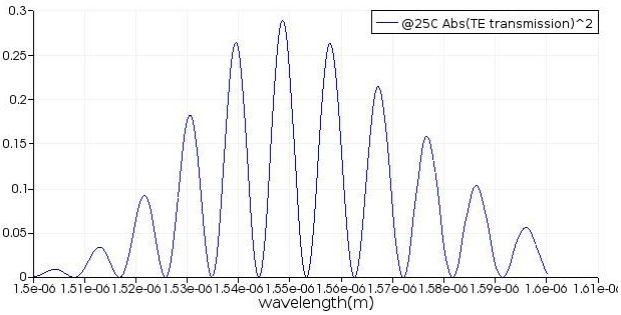

Figure 6. Spectrum of the imbalance MZI with $\Delta L=50\mu m$, TE mode for 500nmx220nm waveguide.

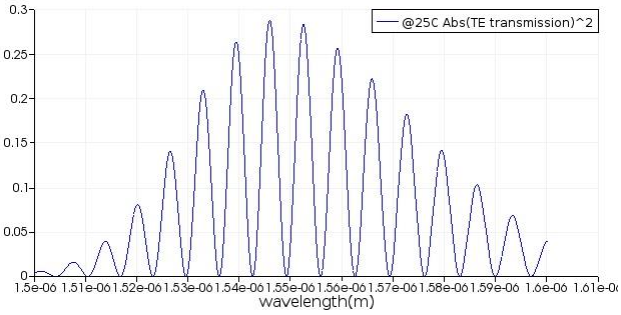

Figure 7. Spectrum of the imbalance MZI with $\Delta L=70\mu m$, TE mode for 500nmx220nm waveguide.

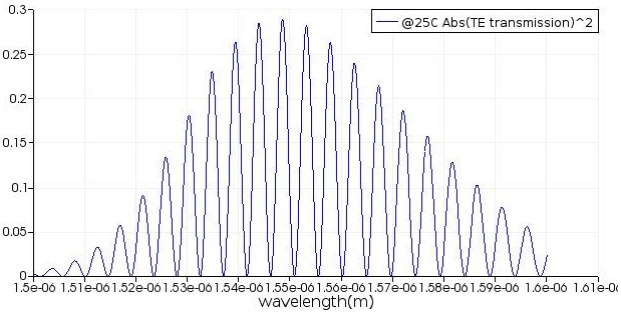

Figure 8. Spectrum of the imbalance MZI with $\Delta L=90\mu m$, TE mode for 500nmx220nm waveguide.

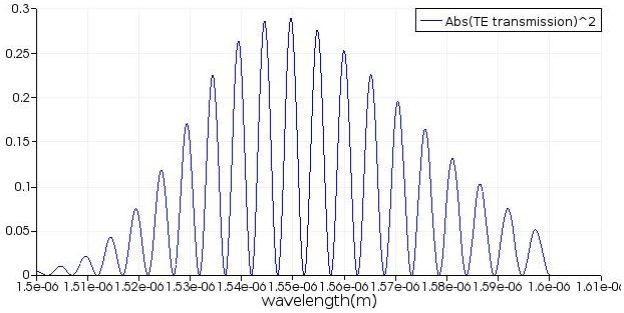

Figure 9. Spectrum of the imbalance MZI with $\Delta L=100\mu m$, TE mode for 500nmx220nm waveguide.

D. Frequency Spectrum Range FSR

The free spectrum range FSR defined as the length between adjacent peaks of the MZI sinusoidal output is

$$FSR=\Delta\lambda=\lambda_{m+1}-\lambda_m \approx \frac{\lambda^2}{\Delta L n_g}. \quad (10)$$

where n_g is the group index defined as

$$n_g = n_{eff}+\nu\frac{dn_{eff}}{d\nu}. \quad (11)$$

IV. Corner Analysis for FSR and n_g

A. *Width and Height variation*

Using Mode solutions we calculated the effect of the width and height parameter variation on FSR and group index. In Mode solution we set a mesh override at the edges for each corner analysis and also we set the maximum mesh step in y and z directions to dy=20nm and dz=5nm. Those maximum values are determined by the convergence tests to make sure that the error in the group index calculation does not exceed 0.01 for the same $1.55\mu m$ wavelength, TE polarization and waveguide geometry 500nm width by 220nm height. For this corner analysis we used Si Palik for the waveguide and wafer and SiO2 with constant refractive index of 1.444 for the cladding. Also in this analysis we ignored bend effects.

The following table summarizes group index results of the nominal and corner analysis.

TABLE 1. TE & TM MODE NOMINAL AND CORNER ANALYSIS.

	TE	TM
Nominal n_g	4.19176	3.72307
Minn_g	4.1702	3.4888
Max n_g	4.24921	3.84185

These group indexes are calculated in Mode solution for a waveguide with 500nm x 220nm geometry using FDE solver settings of dy=20nm, dz=5nm, and four mesh overrides at the edges in y and z directions.

Using the above nominal and corner analysis for the group index n_g, we calculated the expected FSR for the designed MZIs. The result is listed in tables 2 and 3.

TABLE 2. FSR CORNER ANALYSIS FOR TE MODE.

ΔL	FSR_{min}	FSR_{max}
30μm	18.84663	19.20372
50μm	11.30798	11.52223
70μm	8.07713	8.23017
90μm	6.28221	6.40124
100μm	5.65399	5.76112

TABLE 3. FSR CORNER ANALYSIS FOR TM MODE.

ΔL	FSR_{min}	FSR_{max}
30μm	20.84502	22.95444
50μm	12.50701	13.77266
70μm	8.93358	9.83762
90μm	6.94834	7.65148
100μm	6.25351	6.88633

B. Temperature variation impact

Temperature effect is simulated in Lumerical INTERCONNECT. First the effective index temperature coefficient is calculated in Lumerical MODE and found to be 0.000198183 for TE mode, and 0.00010948 for TM mode waveguides. However we used a more conservative temperature coefficient of 0.000198467

Temperature variation impact on transmission, gain FSR and extension ratio is then simulated using an MZI with $\Delta L=90\mu m$, and from Fig. 10,11,12 and 13, we can see the impact of temperature variation on transmission spectrum, gain, FSR and extension ratio. The impact can be summarized as a shift in the spectrum. The change in extension ratio came unexpectedly higher for 35C than 45C and 25C.

V.LAYOUT

The area of the silicon waver is shared between multiple designers, where each designer is assigned a layout area of $605\mu m$ by $410\mu m$. The layout is exported into GDSII format and submitted to the University of British Columbia where all designs from all designers are collected into one single multi project waver MPW and then sent to the fabrication facility at University of Washington. Fig. 14, show the layout design for MZIs with different ΔL

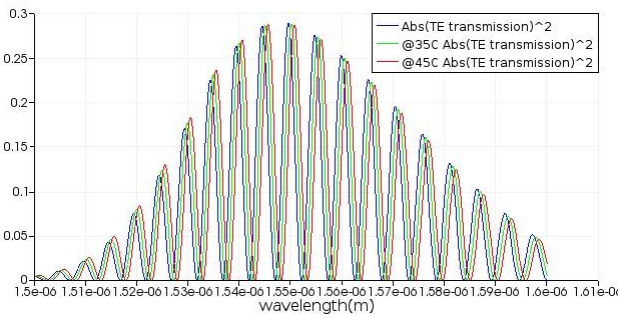

Figure 10. Transmission spectrum temperature variation for imbalance MZI with $\Delta L=90\mu m$, TE mode for 500nmx220nm waveguide.

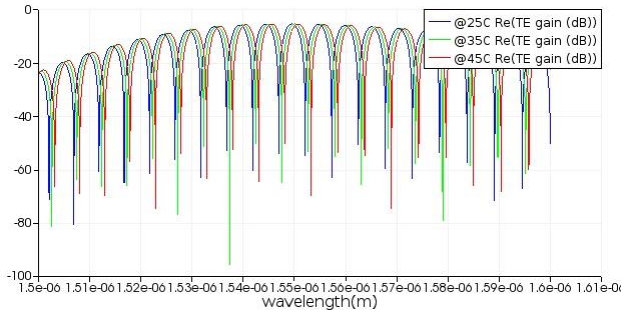

Figure 11. Gain temperature variation for imbalance MZI with $\Delta L=90\mu m$, TE mode for 500nmx220nm waveguide.

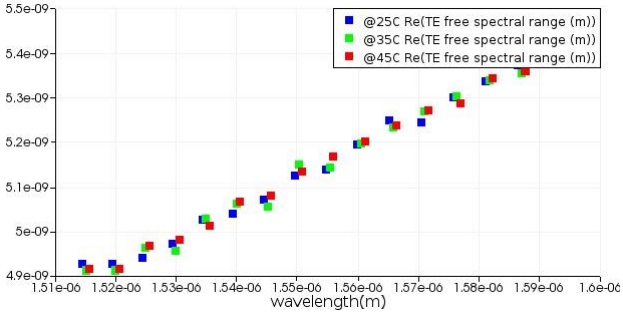

Figure 12. FSR temperature variation for imbalance MZI with $\Delta L=90\mu m$, TE mode for 500nmx220nm waveguide.

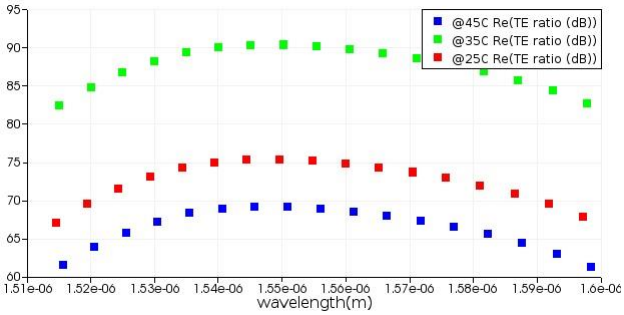

Figure 13. Extension ratio temperature variation for imbalance MZI with $\Delta L=90\mu m$, TE mode for 500nmx220nm waveguide.

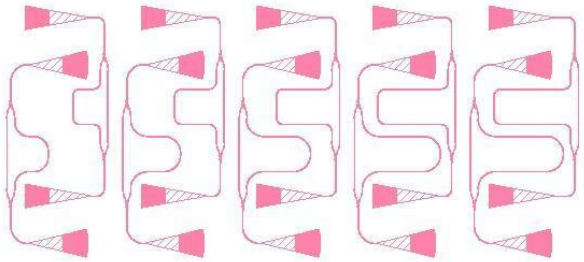

Figure 14. Layout of TE and TM Mode MZIs with $\Delta L=30\mu m$, $\Delta L=50\mu m$, $\Delta L=70\mu m$, $\Delta L=90\mu m$and $\Delta L=100\mu m$

All devices are designed for TE and TM mode and all waveguides are designed with 500nm width and 220nm height. The bends are made $5\mu m$ for TE mode devices and $10\mu m$ for TM mode devices. All components are made using layer 1 with regular 6nm shot pitch.

The components are placed in a compact form with TE and TM circuits back to back so that we can include as many components as possible. However the test setup arrangement at the UBC Ref. [3] has put a constrain on the locations of the grating couplers with fixed $127\mu m$ pitch, this leaves more than 20% of the layout area un used. The devices are placed far away from each other by at least $3\mu m$ to avoid any possible interference or optical crosstalk.

Klayout Ref. [8] is an open source tool we used for editing and creating the layout.

VI. Experimental Data Analysis

Measurements at room temperature 25^oC and non room temperatures 35^oC and45^oC are done. One common issue in the experimental data is that almost all TE mode components suffer from noise particularly at lower wavelength edge. However the higher wavelength edge was clean in almost all components. This is not the case for TM mode devices. Fortunately an embedding components for TE and TM devices are included in the layout, these embedding circuits helps in removing the effect of the grating couplers non flat response however farther analysis is needed to discover in more detail all the sources of this noise and the methods to reduce them. For the current experimental data we used a digital filter to suppress the noise specially at the lower wavelength edge, also a window of the spectrum ranging from $1.54\mu m$ to $1.58\mu m$ is used to measure the group index and the FSR. After setting $\lambda_{min} = 1.54\mu m$ and $\lambda_{max} = 1.58\mu m$, the experimental data was fit to a very good degree. And with auto correlation we measured the FSR and the group index n_g. However for TE mode devices we found these min and max wavelengths range affects the calculated FSR from the measurement data and hence affects the group index as well.

We also observed much cleaner data measurement for all TM mode devices, and this is due mainly to low loss feature of TM mode waveguides. The noise was very small and only at the higher wavelength edge, compared with very noisy measurement data at the lower wavelength edge in the TE mode devices Ref. [6]

Corner analysis for the group index is calculated using Mode solutions with 4 corners, 4 edges and nominal waveguide width and height.

Tables 4 and 5, list the extracted group index and FSR from the measurement data for various MZIs at room temperature and at 35C. The extracted free spectrum range is found using auto correlation technique.

TABLE 4. Group index $n_g$and FSR from measurement data at room temperature. Corner analysis for TM mode.

ΔL	Measured n_g	Measured FSR	Fit goodness
$100\mu m$	4.1731	5.8600e-09	0.9516
$70\mu m$	4.1427	8.3900e-09	0.9755
$30\mu m$	3.9890	1.9630e-08	0.9832

TABLE 5. Group index $n_g$and FSR from measurement data at $35°C$. Corner analysis for TM mode.

ΔL	Measured n_g	Measured FSR	Fit goodness
$100\mu m$	4.1731	5.8800e-09	0.9586
$70\mu m$	4.1486	8.4500e-09	0.9546
$30\mu m$	3.9777	1.9830e-08	0.9930

As mentioned before, one important parameter that affects the above tabulated results for TE mode devices is the spectrum range. The MATLAB calculated results from measurement data can change considerably if we change the range. This is mainly due to noise at the lower wavelength edge however further investigation is needed.

Fig. 15, show MATLAB MZI fitting for a selected MZI device with $\Delta L=90\mu m$, the measured group index n_g is 4.1797 at 1550nm and the FSR is 6.46nm.

Since the TE mode data is very noisy at the lower edge, we need to limit the analysis to a range of spectrum. The curve fitting with autocorrelation MATLAB code is updated by setting $\lambda_{min} = 1.56\mu m$,$\lambda_{max} = 1.6\mu m$ and

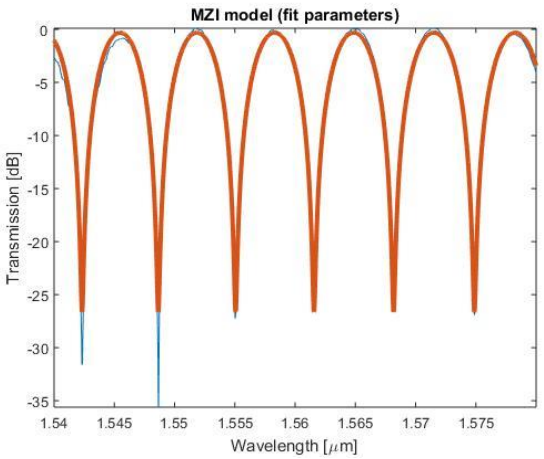

$\lambda_0 = 1.55\mu m$.

Figure 15. Model fit for MZI with $\Delta L=90\mu m$ and 500nmx220nm waveguide in TE mode and at $25°C$.

VII. Fabrication and Measurement Setup

The devices were fabricated using 100 keV Electron Beam Lithography Ref. [1]. The fabrication used silicon-on-insulator wafer with 220 nm thick silicon on 3 µm thick silicon dioxide. The substrates were 25 mm squares diced from 150 mm wafers. After a solvent rinse and hot-plate dehydration bake, hydrogen silsesquioxane resist (HSQ, Dow-Corning XP-1541-006) was spin-coated at 4000 rpm, then hotplate baked at 80 °C for 4 minutes. Electron beam lithography was performed using a JEOL JBX-6300FS system operated at 100 keV energy, 8 nA beam current, and 500 µm exposure field size. The machine grid used for shape placement was 1 nm, while the beam stepping grid, the spacing between dwell points during the shape writing, was 6 nm. An exposure dose of 2800 µC/cm2 was used. The resist was developed by immersion in 25 tetramethylammonium hydroxide for 4 minutes, followed by a flowing deionized water rinse for 60 s, an isopropanol rinse for 10 s, and then blown dry with nitrogen. The silicon was removed from unexposed areas using inductively coupled plasma etching in an Oxford Plasmalab System 100, with a chlorine gas flow of 20 sccm, pressure of 12 mT, ICP power of 800 W, bias power of 40 W, and a platen temperature of 20 °C, resulting in a bias voltage of 185 V. During etching, chips were mounted on a 100 mm silicon carrier wafer using perfluoropolyether vacuum oil.

Measurement description: To characterize the devices, a custom-built automated test setup Ref. [2] with automated control software written in Python was used Ref. [3]. An Agilent 81600B tunable laser was used as the input source and Agilent 81635A optical power sensors as the output detectors. The wavelength was swept from 1500 to 1600 nm in 10 pm steps. A polarization maintaining (PM) fibre was used to maintain the polarization state of the light, to couple the TE polarization into the grating couplers [4]. A 90º rotation was used to inject light into the TM grating couplers Ref. [4]. A polarization maintaining fibre array was used to couple light in/out of the chip Ref. [5].

VIII. Conclusion

In this paper we presented the design and analysis of one useful silicon photonic structure namely Mach Zehnder Interferometer. We modeled an imbalanced MZI using Lumerical tools, and presented simulation results and layout of MZI interferometer, finally we analyzed and compared simulated data with the measurement data. The measured group index came within the expected corner analysis range, however we found that due to noise at the lower wavelength edge we must trim the spectrum range to $\lambda_{min} = 1.54\mu m$, $\lambda_{max} = 1.58\mu m$ and these min and max wavelengths range affects the calculated FSR from the measurement data and hence affects the group index as well.

Acknowledgment

I acknowledge the edX UBCx Silicon Photonics Design, Fabrication and Data Analysis course, which is supported by the Natural Sciences and Engineering Research Council of Canada (NSERC) Silicon Electronic-Photonic Integrated Circuits (SiEPIC) Program. The devices were fabricated by Richard Bojko at the University of Washington Washington Nanofabrication Facility, part of the National Science Foundation's National Nanotechnology Infrastructure Network (NNIN). Zeqin Lu performed the measurements at The University of British Columbia. We acknowledge Lumerical Solutions, Inc., Mathworks, Mentor Graphics, Python, and KLayout for the design software.

References

[1] R. J. Bojko, J. Li, L. He, T. Baehr-Jones, M. Hochberg, and Y. Aida, "Electron beam lithography writing strategies for low loss, high confinement silicon optical waveguides," J. Vacuum Sci. Technol. B 29, 06F309 (2011)

[2] Lukas Chrostowski, Michael Hochberg, chapter 12 in "Silicon Photonics Design: From Devices to Systems", Cambridge University Press, 2015

[3] URL:http://siepic.ubc.ca/probestation, using Python code developed by Michael Caverley.

[4] Yun Wang, Xu Wang, Jonas Flueckiger, Han Yun, Wei Shi, Richard Bojko, Nicolas A. F. Jaeger, Lukas Chrostowski, "Focusing sub-wavelength grating couplers with low back reflections for rapid prototyping of silicon photonic circuits", Optics Express Vol. 22, Issue 17, pp. 20652-20662 (2014) doi: 10.1364/OE.22.020652

[5] www.plcconnections.com, PLC Connections, Columbus, OH.

[6] M. Drebi, "Silicon Photonics Design, Fabrication and Data Analysis," edX Phot1x proposal report 2015.

[7] Lumerical Solutions Inc., Innovative Photonic Design Tools, URL:http://www.lumerical.com

[8] KLayout Layout Viewer and Editor. URL:http://www.klayout.de

Biographies

Muharrem Drebi received his B.Sc. degree from the University of Tripoli, and M.Sc. degree from the University of Washington. Muharrem worked in the past as circuit design engineer at Intel Corp., Oregon design center where he participated in the design and validation of many Microprocessor design projects. Currently he is a full staff member and a lecturer at the University of Tripoli, department of computer engineering, he is also working as coordinator for students B.Sc. projects. In 2014, Muharrem was nominated by the engineering college and received a full higher education scholarship to pursue PhD study abroad pending financial support. Muharrem research interests include mixed signal circuit design, photonic integrated circuits, nanoelectronics and quantum computing.